New Materials, Compounds and Applications
Vol.2, No.3, 2018, pp.221-230

Tl_2Te-Tl_9SbTe_6-Tl_9TbTe_6 SYSTEM

Samira Z. Imamaliyeva[1*], Ganira I. Alakbarova[2,3], Kamala N. Babanly[1], Imameddin R. Amiraslanov[4], Mahammad B. Babanly[1]

[1]Institute of Catalysis and Inorganic Chemistry named after acad. M. Nagiyev, Azerbaijan National Academy of Sciences, Baku, Azerbaijan
[2]Azerbaijan State Oil and Industry University, Baku, Azerbaijan
[3]National Aerospace Agency of Azerbaijan Republic, Baku, Azerbaijan
[4]Institute of Physics, Azerbaijan National Academy of Sciences, Baku, Azerbaijan

Abstract. Phase relations of the Tl-Sb-Tb-Te quaternary system in the Tl_2Te-Tl_9SbTe_6-Tl_9TbTe_6 section were experimentally studied by using the differential thermal analysis, powder X-ray diffraction technique, and microhardness measurements. Several polythermal sections, an isothermal sections at 300 and 740 K, and projections of the liquidus and solidus surfaces were constructed. A wide areas of solid solutions with a Tl_5Te_3 structure, which are of interest as potential thermoelectric materials, is formed in the system.

Keywords: *thallium-antimony tellurides, thallium-terbium tellurides, phase relations, projections of the liquids, solid solutions, crystal structure.*

Corresponding Author: *Samira Imamaliyeva, Institute of Catalysis and Inorganic Chemistry named after acad. M. Nagiyev, Azerbaijan National Academy of Sciences, 113, H. Javid. ave., AZ-1143, Baku, Azerbaijan, e-mail: samira9597a@gmail.com*

Received: *2 October 2018;* ***Accepted****: 16 November 2018;* ***Published:*** *17 December 2018.*

1. Introduction

Materials based on multinary chalcogenides are essential due to their functional properties like as optic, photoelectric, magnet, thermoelectric, topological insulators et al. (Kolobov & Tominaga, 2016; Ahluwalia, 2017; Alonso-Vante, 2018; Scheer & Schock, 2011; Ghang *et al.*, 2014; Macia, 2015; Gao *et al.*, 2013; Duan *et al.*, 2015; Papagno *et al.*, 2016; Okamoto *et al.*, 2012).

Thallium subtelluride, Tl_5Te_3 due to features of its crystal structure, is suitable "matrix" for the fabrication of novel complex materials (Schewe *et al.*, 1989; Bhan & Schubert, 1970). Such materials include $Tl_4A^{IV}Te_3$ and $Tl_9B^{V}Te_6$ -type (A^{IV}-Sn, Pb; B^{V}-Sb, Bi) compounds (Gotuk *et al.*, 1979; Babanly *et al.*, 1985a, b) which also possess a good thermoelectric performance (Guo *et al.*, 2013; 2014; Yamanaka *et al.*, 2003). Moreover, the Dirac-like surface states in the Tl_5Te_3 and its non-superconducting derivative $[Tl_4](Tl_{1-x}Sn_x)Te_3$ was found by authors of Ref. (Arpino *et al.*, 2015).

Earlier Babanly and coauthors (Babanly *et al.*, 2009; Imamaliyeva *et al.*, 2008) showed the formation of a new class of ternary cation-substituted structural analogs of Tl_5Te_3 with common formula Tl_9LnTe_6 (Ln-Ce, Nd, Sm, Gd, Tb, Tm). It was also showed that ytterbium does not form the compound of Tl_9YbTe_6-type that apparently associated with the stability of the electronic configuration of the ytterbium atom (Imamaliyeva *et al.*, 2015). A little later these results were confirmed (Bangarigadu-

Sanasy *et al.*, 2011, 2013, 2014), which and determined the thermoelectric and magnetic properties for a number Tl_9LnTe_6-type compounds.

The design and development of novel methods for controlled synthesis and growth of large single crystals requiredetailed studies of respective phase diagrams and the thermodynamic functions (Zlomanov *et al.*, 2013; Tomashyk, 2016). On other hand, according to Ioffe (Ioffe, 1957), incorporation of the heavy atoms into crystal lattice can improve their thermoelectric properties and give them additional functionality. For this purpose, the phase equilibria of a number of systems including compounds with the Tl_5Te_3 structure (Imamaliyeva *et al*., 2017a, b, c, 2018) were investigated. As a result, it was shown that these systems are characterized by the formation of continuous series of solid solutions.

This study reports a detailed experimental investigation of the phase equilibria in the Tl_2Te-Tl_9SbTe_6-Tl_9TbTe_6 section of the Tl-Sb-Tb-Te quaternary system.

Tl_2Te and Tl_9SbTe_6 compounds melt congruently at 698 (Asadov *et al.*, 1977) and 800 K (Borgros, 1977), while Tl_9TbTe_6 melts with decomposition by the peritectic reaction at 780 K (Imamaliyeva *et al*., 2017a). Tl_2Te crystallizes in the monoclinic system (sp.gr. *C*2/*c*; a = 15.662; b = 8.987; c=31.196Å, β=100.76^0, z=44) (Cerny *et al.*, 2002). The tetragonal lattice parameters of Tl_9SbTe_6 and Tl_9TbTe_6 are equal: a = 8.829, c = 13.001 Å, z=2 (Wacker, 1991); a=8.871, c=12.973, z=2 (Imamaliyeva *et al.*, 2017a).

Tl_9SbTe_6-Tl_9TbTe_6 and Tl_2Te-Tl_9TbTe_6 sections are non-quasi-binary due to peritectic melting of Tl_9TbTe_6 (Imamaliyeva *et al*., 2017a, d). The first system is characterized by the formation of continuous series of solid solutions while second section by limited solid solutions.

There are 2 variants of the phase diagram of the system Tl_2Te-Tl_9SbTe_6 in the literature. According to Botgros (Botgros *et al.*, 1977), the system is characterized by the formation of a continuous series of solid solutions. According to the data of (Babanly *et al.*, 1985), there is a morphotropic phase transition in solid solutions near Tl_2Te. Taking into account that the Tl_2Te and Tl_9SbTe_6 compounds have completely different crystalline structures, this statement seems unlikely. Considering this, we reinvestigated the Tl_2Te-Tl_9SbTe_6 system.

2. Experimental

2.1. Materials and syntheses

For samples preparation we used high purity elements: thallium (99.999%), antimony (99.999 %), terbium (99.9%), and tellurium (99.999%). All the elements were purchased from Alpha Aesar Company. Because thallium is stored in water, it was dried and the oxide film was removed before use. We used protective gloves at all times when working with thallium because thallium and its compounds are highly toxic and contact with skin is dangerous.

Stoichiometric amounts of the initial elements were weighed with accuracy ±0.0001 g, put into silica tubesof about 20 cm in length and then were sealed under a vacuum of 10^{-2} Pa.

Tl_2Te and Tl_9SbTe_6 compounds were synthesized by heating in a resistance furnace at 850 K followed by cooling in the switched-off furnace.

The synthesis of the Tl_9TbTe_6 compound was carried out at 1000 K. The intermediate ingot of Tl_9TbTe_6 was carefully powdered in an agate mortar, pressed into

a pellet and annealed at 750 K within ~800 h. because an equilibrium state could not be obtained even after the long-time. We deposited a thin layer of carbon on the inner side of a quartz tube with the aim of to avoid reaction between the terbium and the quartz ampoule.

The purity of the synthesized Tl_2Te, Tl_9SbTe_6, and Tl_9TbTe_6 compounds was monitored by the DTA and XRD techniques.

We observed only one endothermic effect for Tl_2Te (695 K) and Tl_9SbTe_6 (800 K) and two effects for Tl_9TbTe_6 which correspond to the peritectic reaction at 780 K and its liquidus at 1120 K.

Powder XRD data showed that all the samples are phase-pure. Their patterns were indexed using Topas V3.0 software. The obtained unit cell parameters werein good agreement with relevant literature data (Asadov *et al.*, 1977; Imamaliyeva *et al.*, 2017a; Wacker, 1991) (Table 1).

Pre-synthesized compounds were used for the preparation of the samples of the Tl_2Te-Tl_9SbTe_6-Tl_9TbTe_6 system. After synthesis the samples containing >60% Tl_9TbTe_6 were carefully powdered, mixed, pressed into pellets and annealed at 680 K during ~ 800 h in order to complete the homogenization. The mass of each sample was about 1 g.

2.2. Methods

The samples were analyzed by X-ray diffraction and differential thermal analysis as well as microhardness measurements.

The phase identification of powdered specimen was performed using a Bruker D8 diffractometer (CuK_α radiation) at room temperature in the 2θ range of 6–75°. The unit cell parameters of initial compounds and intermediate samples were calculated by indexing of powder patterns using Topas V3.0 software. An accuracy of the crystal lattice parameters is shown in parentheses (Table).

Table 1. DTA data, microhardness values and crystal lattice parameters for some samples of the Tl_2Te-Tl_9SbTe_6-Tl_9TbTe_6 system

Phase	Thermal effects, K	Microhardness, MPa	Lattice parameters, Å
Tl_2Te	695	1400	a = 15.662(8); b = 8.987(4); c = 31.196(12), β = 100.760, z = 44
$Tl_{9,95}Sb_{0,05}Te_{5,05}$	702	1515	-
$Tl_{9,9}Sb_{0,1}Te_{5,1}$	702-715	1330; 1520	-
$Tl_{9,8}Sb_{0,2}Te_{5,2}$	708-728	1320	a = 8.9098(4); c = 12.6792(10)
$Tl_{9,6}Sb_{0,4}Te_{5,4}$	727-753	1270	a = 8.8889(5); c = 12.7604(9)
$Tl_{9,5}Sb_{0,5}Te_{5,}$	740-762	-	-
$Tl_{9,4}Sb_{0,6}Te_{5,6}$	750-773	1180	a = 8.8690(4); c = 12.8416(9)
$Tl_{9,2}Sb_{0,8}Te_{5,8}$	775-790	1100	a = 8.8490(3); c = 12.9228(9)
Tl_9SbTe_6	800	1000	a = 8.8301(2); c = 13.0039(10)

The temperatures of the thermal effects were determined by using a NETZSCH 404 F1 Pegasus differential scanning calorimeter in the range of temperatures from the room temperature to ~1400 K at a heating rate of 10 K· min^{-1} and accuracy about $\pm 2^0$.

Microhardness measurements were done with a microhardness testerPMT-3, the typical loading being 20 g and accuracy about 20 MPa.

3. Results and discussion

An analysis of experimental results and data on boundary systems (Babanly *et al.*, 1985a; Botgros, *et al*, 1977; Imamaliyeva et al., 2017a) enabled us to refine the phase diagram Tl_2Te-Tl_9SbTe_6 and to construct the diagram of the phase relations in the Tl_2Te-Tl_9SbTe_6-Tl_9TbTe_6 system (Table 1, Fig.1-6).

The **Tl_2Te-Tl_9SbTe_6** system (Fig. 1) is quasi-binary and forms a phase diagram of the peritectic type. The coordinates of the L+δ↔α peritectic equilibrium are 5 mol% Tl_9SbTe_6 and 702 K (α- and δ- are solid solutions based on Tl_2Te и Tl_9SbTe_6, respectively). α- and δ- phases are separated by a two-phase region α+δ.

At the peritectic temperature, the homogeneity region of Tl_2Te is about 7 mol%, and for Tl_9SbTe_6 ~85 mol%. With decreasing temperature, these regions narrow somewhat and according to the microhardness measurements and XRD data they are ~5 mol% and ~75 mol%, respectively at 300 K.

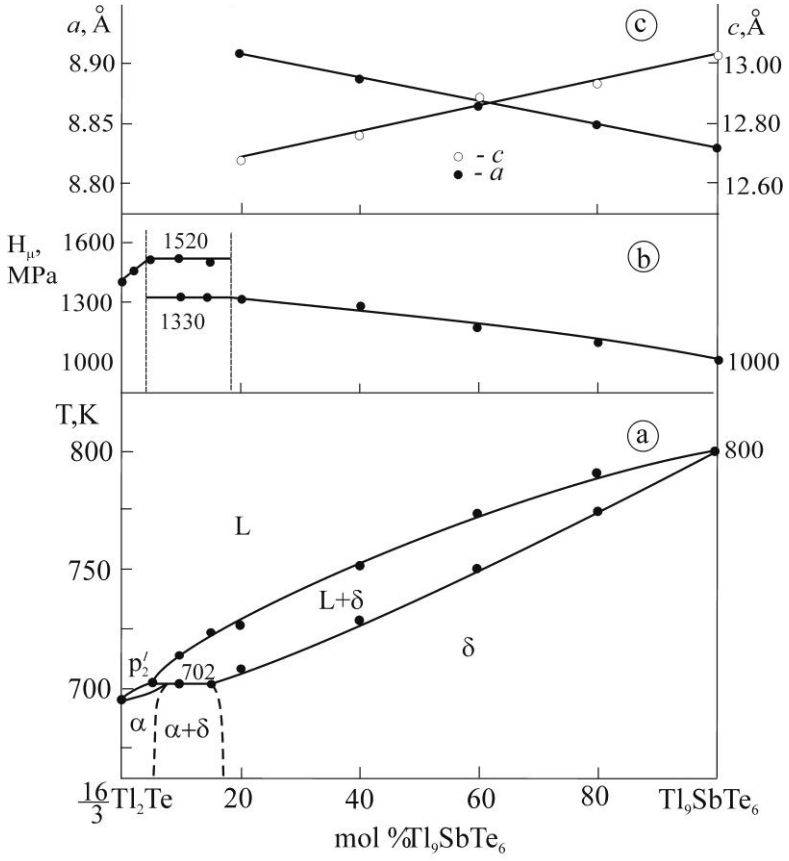

Figure 1. Phase diagram, microhardness values and crystal lattice parameters for the samples of the Tl_2Te-Tl_9SbTe_6 system

Powder XRD results confirm the wide regions of solid solutions in the Tl_2Te-Tl_9SbTe_6 system (Fig.2). The alloys with compositions ≥ 20 mol% Tl_9SbTe_6 are monophasic with Tl_5Te_3-type diffraction patterns. For example, the diffraction pattern 3 presents a pattern with composition 20 mol% Tl_9SbTe_6. Alloys containing 10-15 mol% Tl_9SbTe_6 is bi-phasic (diffraction pattern 2) and besides the δ-phase reflections contains

reflections of α-phase based on Tl_2Te (diffraction pattern 2). Solid solutions containing more than 20 mol% Tl_9SbTe_6 obey the Vegard's law (Fig.1,c) (Ferey, 2017).

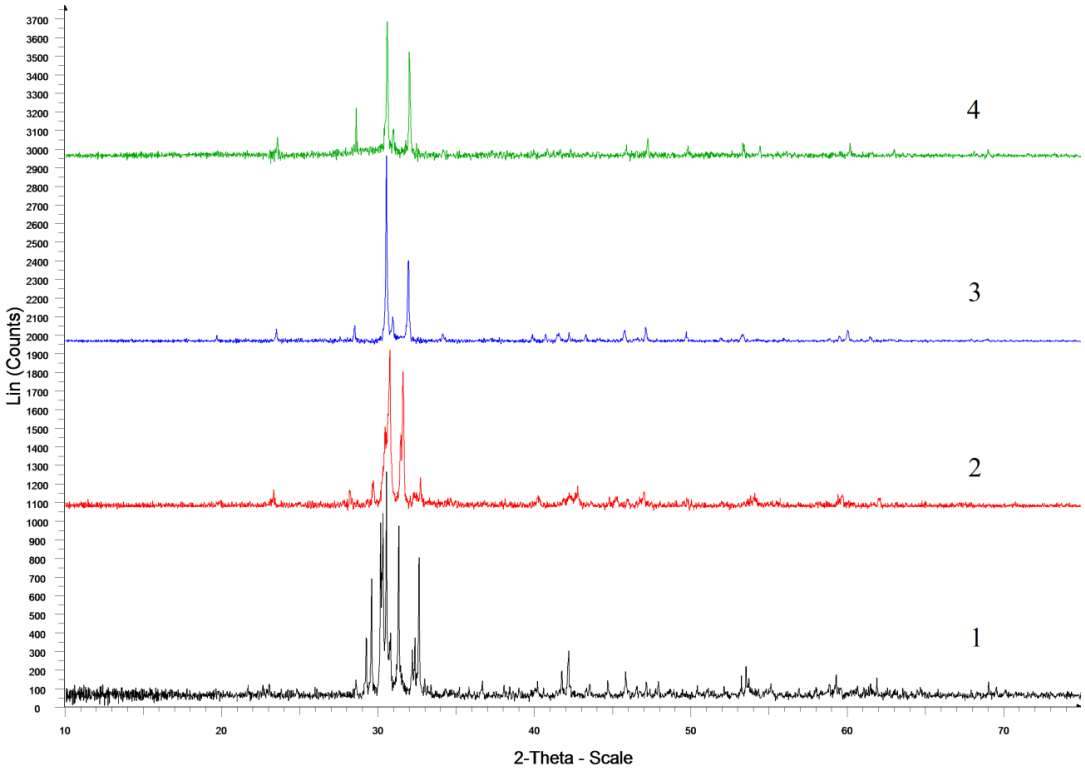

Figure 2. XRD patterns for different compositions in the Tl_2Te Tl_9SbTe_6 system.
1- Tl_2Te; 2- 15mol% Tl_9SbTe_6; 3-20 mol% Tl_9SbTe_6; 4-Tl_9SbTe_6

Microhardness measurements are in good agreement with plotted phase diagram (Fig.1, b). The microhardness values of initial compounds are increased within homogeneity areas of α- and δ-phases, and remain constant in the α+δ two-phase region (Glazov, 1969).

The solid-phase equilibria diagram

This diagram (Fig. 3) clearly demonstrates the location of the phase regions in the Tl_2Te -Tl_9TbTe_6-Tl_9SbTe_6 system at room temperature. As can be seen, the system consists of two single-phase fields (α- and δ-), limited by α+δ two-phase region. Fig.3. presents the studied sections and alloys compositions.

The liquidus surface projection (Fig. 4)

Liquidus of Tl_2Te-Tl_9SbTe_6-Tl_9TbTe_6 section consists of three areas of the primary crystallization of α-,δ-phases and $TlTbTe_2$ compound. These areas are limited by lines of p_1p_1' and p_2p_2' which correspond to the monovariant peritectic equilibria L+ $TlTbTe_2 \leftrightarrow \delta$ and $L+\delta \leftrightarrow \alpha$. Solidus surface consists of two areas corresponding to the completion of crystallization α- and δ-phases.

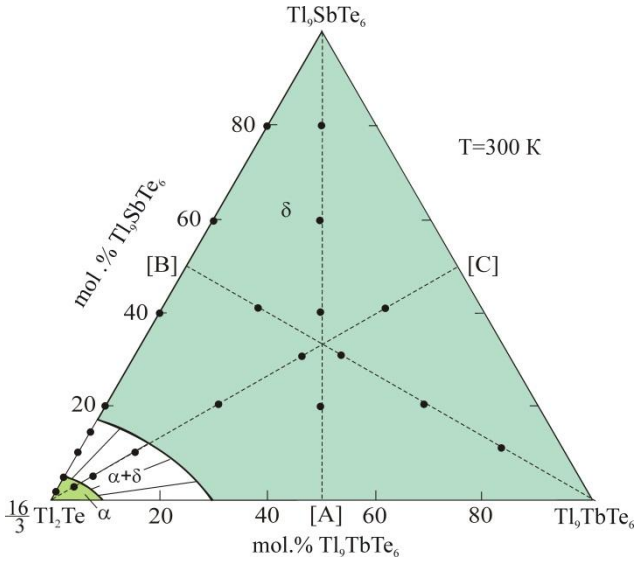

Figure 3. The solid-phase diagram of the Tl_2Te-Tl_9SbTe_6-Tl_9TbTe_6section. The studied sections (das-dot lines) and alloys compositions (circles) are shown

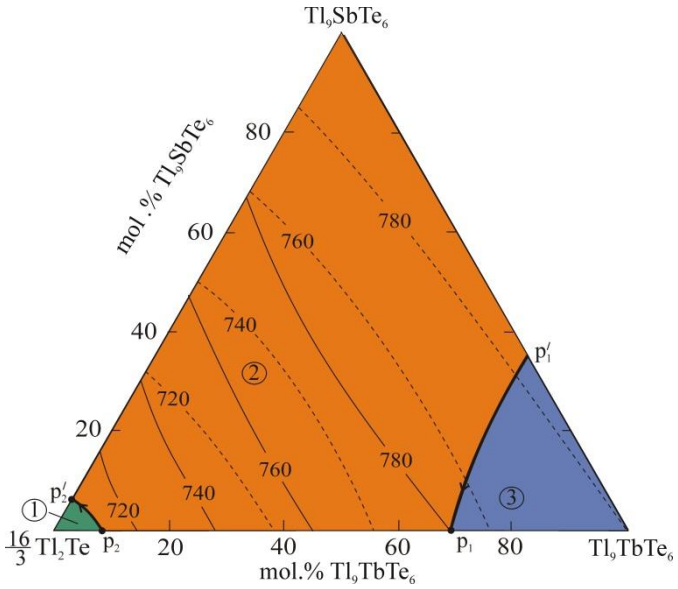

Figure 4. Projection of the liquidus and solidus (dashed lines) surface of the Tl_2Te-Tl_9TbTe_6-Tl_9SbTe_6 system. Primary crystallization fields of phases: 1-α; 2-δ; 3- $TlTbTe_2$.

Polythermal sections of the Tl_2Te-Tl_9SbTe_6-Tl_9TbTe_6 system (Fig.5)

Figs. 5a-c show the polythermal sections $2Tl_2Te$-[C], Tl_9SbTe_6-[A] and Tl_9TbTe_6-[B] of the Tl_2Te-Tl_9SbTe_6-Tl_9TbTe_6 system, where A, B, and C are equimolar compositions on the boundary systems as shown in Fig.3.

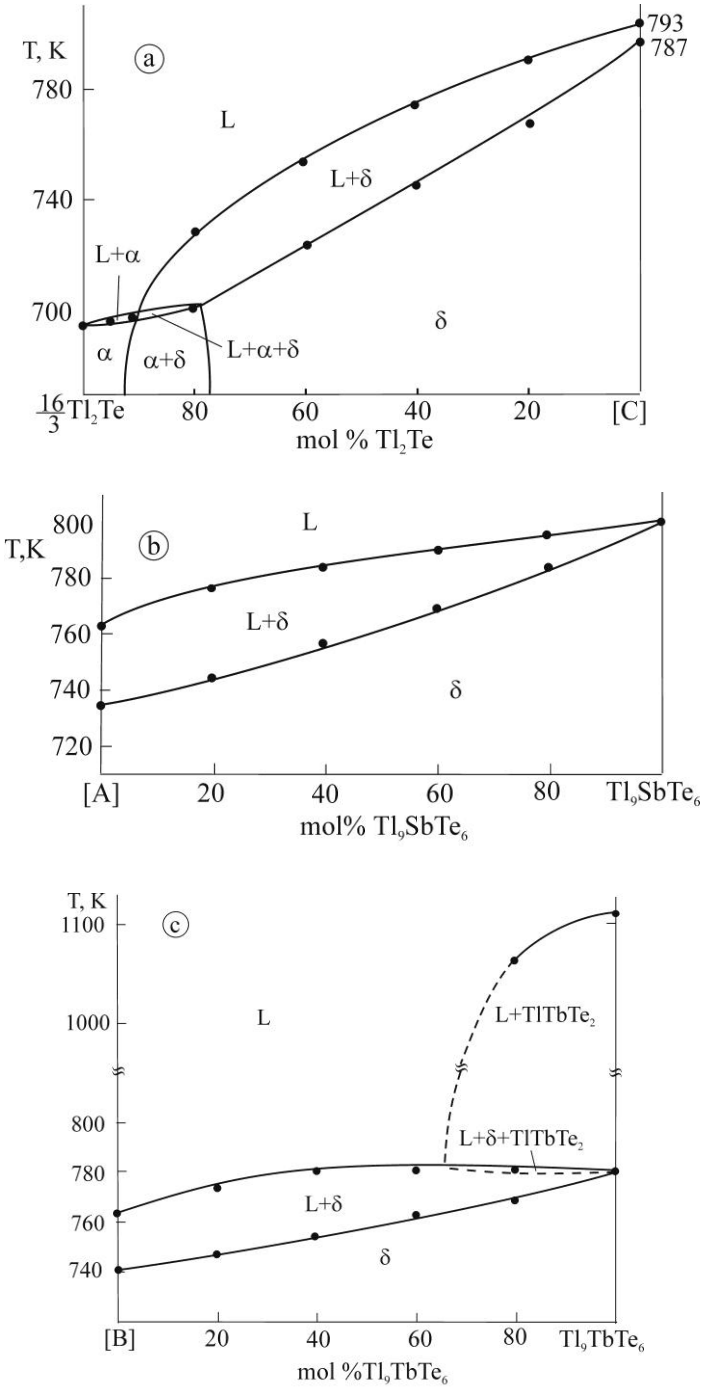

Fig.5. Polythermal sections Tl_2Te-[A], Tl_9SbTe_6-[B] and Tl_9TbTe_6-[C] of the phase diagram of the Tl_2Te -Tl_9TbTe_6-Tl_9SbTe_6 system

The liquidus of Tl_2Te-[C] section consists of two curves of primary crystallization of α- and δ-phases. The intersection point of these curves corresponds to the monovariant peritectic reaction L+δ↔α (702 K). This section passes through the α, α+δ and δ- phase areas below the solidus.

The δ-phase crystallizes from the Tl_9SbTe_6-[A] section over the entire compositions interval from the melt (Fig.5, b).

The δ-phase crystallizes from the Tl_9TbTe_6-[B] section in the composition range

up to ~65 mol% of Tl_9TbTe_6, whereas in the Tl_9TbTe_6- rich alloys, the $TlTbTe_2$ compound first crystallizes (Imamaliyeva *et al*., 2017a), then the monovariant peritectic equilibrium L+ $TlTbTe_2 \leftrightarrow \delta$ occurs. In the latter reaction, the $TlTbTe_2$ is completely consumed first and the excess of the melt crystallizes into the δ- phase.

Isothermal section at 740 K (Fig. 6)

The isothermal section of the phase diagram at 740 K is presented on Fig.6. As can be seen, the connods are practically radial from the Tl_2Te coner of the concentration triangle, which is associated with the proximity of the melting temperatures of Tl_9TbTe_6 and Tl_9SbTe_6.

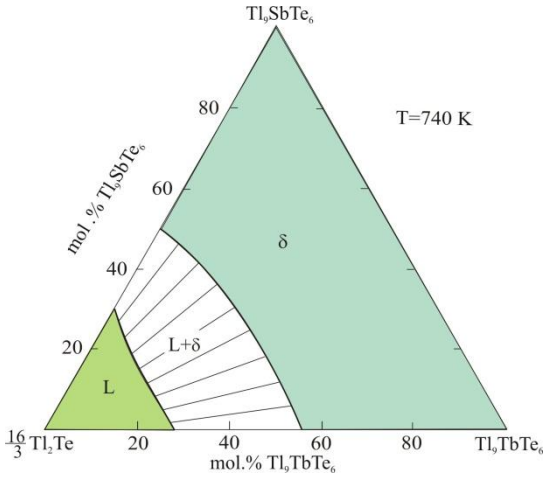

Figure 6. The isothermal section of the phase diagram of the Tl_2Te-Tl_9SbTe_6-Tl_9TbTe_6 system at 740 K.

4. Conclusion

A full T-x-y diagram of the Tl_2Te-Tl_9SbTe_6-Tl_9TbTe_6system, including the phase diagrams of boundary system Tl_2Te-Tl_9SbTe_6, some polythermal sections, an isothermal section at 300 and 740 K, and the liquidus and solidus surface projections were constructed. It was found that wide areas of δ-solid solutions with the Tl_5Te_3 structure occupy more than 90% of the concentration triangle. Obtained experimental data can be used for choosing the composition of solution-melt and for determining of temperature conditions for growing crystals of δ- phase with a given composition.

Acknowledgment

This work was supported by the Science Development Foundation under the President of the Republic of Azerbaijan – Grant № EIF/MQM/Elm-Tehsil-1-2016-1(26)-71/01/4-M-33.

References

Alonso-Vante, N. (2018). *Chalcogenide Materials for Energy Conversion: Pathways to Oxygen and Hydrogen Reactions*. Springer.

Ahluwalia, G.K. (2017). *Applications of chalcogenides: S, Se, and Te*. Springer International Publishing.

Arpino, K.E., Wasser, B.D. & McQueen, T.M. (2015). Superconducting dome and crossover to an insulating state in $[Tl_4]$ $Tl_{1-x}Sn_xTe_3$. *APL materials*, *3*(4), 041507.

Asadov, M.M., Babanly, M.B. &Kuliev, A.A. (1977). Phase equilibria in the Tl-Te system. *Inorg.Mater.*, *13*(8), 1407-1410.

Babanly, M.B., Azizulla, A. & Kuliev, A.A. (1985a).System Tl_2Te-Bi_2Te_3-Te. *Russ. J. Inorg. Chem.*, *30*(9), 2356-2359.

Babanly, M.B., Azizulla, A. & Kuliev, A.A. (1985b). System Tl-Sb-Te. *Russ. J. Inorg. Chem.*, 30, 1051-1059.

Babanly, M.B., Imamalieva, S.Z., Babanly, D.M. & Sadygov, F.M. (2009). Tl_9LnTe_6 (Ln = Ce, Sm, Gd) compounds— new structural analogs of Tl_5Te_3. *Azerb.Chem.J.*, 1, 122–125.

Bangarigadu-Sanasy, S., Sankar, C. R., Assoud, A. & Kleinke, H. (2011). Crystal structures and thermoelectric properties of the series $Tl_{10-x}La_xTe_6$ with $0.2 \leq x \leq 1.15$. *Dalton Transactions*, *40*(4), 862-867.

Bangarigadu-Sanasy, S., Sankar, C.R., Dube, P.A., Greedan, J.E. & Kleinke, H. (2014). Magnetic properties of Tl_9LnTe_6, Ln= Ce, Pr, Tb and Sm. *Journal of Alloys and Compounds*, *589*, 389-392.

Bangarigadu-Sanasy, S., Sankar, C.R., Schlender, P. & Kleinke, H. (2013). Thermoelectric properties of $Tl_{10-x}Ln_xTe_6$,with Ln = Ce, Pr, Nd, Sm, Gd, Tb, Dy, Ho and Er, and $0.25<x<1.32$. *J. Alloy. Com.*, 549, 126–134.

Bhan, S. & Schubert, K. (1970).Kristallstruktur von Tl_5Te_3 und Tl_2Te_3. *Journal of the Less Common Metals*, *20*(3), 229-235.

Botgros, I.V., Zbigli K.R., Stanchu, A.V., Stepanov, G.I. & Chumak, G.D. (1977). Section Tl_2Te-Sb_2Te_3 of the system Tl-Sb-Te. *Inorg.Mater.*, *13*(7), 1202-1210.

Černý, R., Joubert, J.M., Filinchuk, Y. & Feutelais, Y. (2002). Tl_2Te and its relationship with Tl5Te3. *Acta Crystallographica Section C: Crystal Structure Communications*, *58*(5), i63-i65.

Chang, Sh-H., Parinov, I.A., Topolov,V.Yu. (2014). *Advanced Materials*, Springer International Publishing.

Duan, X., Wang, C., Pan, A., Yu, R. & Duan, X. (2015). Two-dimensional transition metal dichalcogenides as atomically thin semiconductors: opportunities and challenges. *Chemical Society Reviews*, *44*(24), 8859-8876.

Férey, G. (2017). *Crystal Chemistry: From Basics to Tools for Materials Creation*.

Gao, M.R., Xu, Y.F., Jiang, J. & Yu, S.H. (2013). Nanostructured metal chalcogenides: synthesis, modification, and applications in energy conversion and storage devices. *Chemical Society Reviews*, *42*(7), 2986-3017.

Glazov, V.M. & Vigdorovich, V.N. (1969). *Microhardness of Metals and Semiconductors*. Corrected and Supplemented (in Russian).

Gotuk, A.A., Babanly, M.B. & Kuliev, A.A. (1979). Phase equilibria in the system Tl-Sn-Te. *Inorg.Mater.*, 15, 1062-1067.

Guo, Q., Chan, M. & Kuropatwa, B.A. (2013). Enhanced thermoelectric properties of variants of Tl_9SbTe_6 and Tl_9BiTe_6. *Chem. Mater.*, *25*(20), 4097–4104.

Guo, Q., Chan, M., Kuropatwa, B.A. & Kleinke, H. (2014).Thermoelectric properties of Sn-and Pb-doped Tl_9BiTe_6 and Tl_9SbTe_6. *Journal of Applied Physics*, *116*(18), 183702.

Imamalieva, S.Z., Sadygov, F.M. & Babanly, M.B. (2008). New thallium neodymium tellurides. *Inorganic Materials*, *44*(9), 935.

Imamaliyeva, S.Z. (2018). Phase diagrams in the development of thallium-REE tellurides with Tl_5Te_3 structure and multicomponent phases based on them. *Condensed matter and interphases*, 20(3), 332-347.

Imamaliyeva, S.Z., Gasanly, T.M., Amiraslanov, I.R. & Babanlı, M.B. (2017a). Phase relations in the Tl_5Te_3-Tl_9SbTe_6-Tl_9TbTe_6 system. *Chem.Chem.Technol.*, *11*(4), 415-419.

Imamaliyeva, S.Z., Gasanly, T.M., Gasymov, V.A. & Babanlı, M.B. (2017b). Phase equilibria and some properties of solid solutions in the Tl_5Te_3-Tl_9SbTe_6-Tl_9GdTe_6 system. *Acta Chimica Slovenia*, *64*(1), 221–226.

Imamaliyeva, S.Z., Gasanly, T.M., Zlomanov, V.P. & Babanly, M.B. (2017c). Phase equilibria in the Tl_2Te-Tl_5Te_3-Tl_9TbTe_6 system. *Inorg. Mater., 53*(4), 354–361.

Imamaliyeva, S.Z., Mashadiyeva, L.F., Zlomanov, V.P. & Babanly, M.B. (2015). Phase equilibria in the Tl_2Te-YbTe-Te system. *Inorg. Mater., 51*(12), 1333-1338

Imamaliyeva, S.Z., Mekhdiyeva, I.F., Gasymov, V.A.,& Babanlı, M.B. (2017d). Phase equilibria in the Tl_5Te_3-Tl_9BiTe_6-Tl_9TmTe_6 section of the Tl-Bi-Tm-Te quaternary system. *Mater. Res., 20*(4), 1057-1062.

Ioffe, A.F. (1957). *Semiconductor Thermoelements and Thermoelectric Cooling*, London: Infosearch.

Kolobov, A.V. & Tominaga, J. (2016). Introduction.In *Two-Dimensional Transition-Metal Dichalcogenides* (pp. 1-5).Springer, Cham.

Maciá, E. (2015). *Thermoelectric Materials: Advances and Applications*. Pan Stanford.

Okamoto, K., Kuroda, K., Miyahara, H., Miyamoto, K., Okuda, T., Aliev, Z.S. ... & Taniguchi, M. (2012). Observation of a highly spin-polarized topological surface state in $GeBi_2Te_4$. *Physical Review B, 86*(19), 195304.

Papagno, M., Eremeev, S.V., Fujii, J., Aliev, Z.S., Babanly, M.B., Mahatha, S.K. ... & Chulkov, E.V. (2016). Multiple coexisting Dirac surface states in three-dimensional topological insulator $PbBi_6Te_{10}$. *ACS Nano, 10*(3), 3518-3524.

Scheer, R. & Schock, H.W. (2011). *Chalcogenide photovoltaics: physics, technologies, and thin film devices*. John Wiley & Sons.

Schewe, I., Böttcher, P. & Schnering, H.V. (1989). The crystal structure of Tl5Te3 and its relationship to the Cr_5B_3 type. *Zeitschrift für Kristallographie-Crystalline Materials, 188*(1-4), 287-298.

Tomashyk, V.N. (2016). *Multinary Alloys Based on III-V Semiconductors*. RC Press.

Wacker, K. (1991). Die Kristalstrukturen von Tl_9SbSe_6 und Tl_9SbTe_6. *Zeitschrift fuer Kristallographie, Supplement*, 3, 281.

Yamanaka, S., Kosuga, A. & Kurosaki, K. (2003). Thermoelectric properties of Tl_9BiTe_6. *Journal of alloys and compounds, 352*(1-2), 275-278.

Zlomanov, V.P., Khoviv, A.M. & Zavrazhnov, A.J. (2013). Physicochemical Analysis and Synthesis of Nonstoichiometric Solids. In *Materials Science-Advanced Topics*. InTech.